8.3 THE ROLE OF ANTECEDENT PRECIPITATION IN THE DEVELOPMENT OF THE 24–25 JANUARY 2000 U.S. EAST COAST SNOWSTORM

Michael J. Brennan* and Gary M. Lackmann
North Carolina State University, Raleigh, North Carolina

1. INTRODUCTION AND BACKGROUND

The relationship between diabatic processes, such as latent heat release (LHR), and extratropical cyclogenesis has been well documented in the literature (e.g. Tracton 1973; Bosart 1981). This relationship is conveniently viewed through the framework of potential vorticity (PV). The principles of PV conservation and invertibility discussed by Hoskins et al. (1985) allow one to recover balanced atmospheric fields from inverting a portion of the PV field. The impact of non-conservative processes, such as diabatic heating, can be quantified through non-advective PV tendencies.

From the PV perspective, cyclogenesis can be viewed as the mutual interaction of finite-amplitude disturbances at the tropopause and the surface (Hoskins et al. 1985). Latent heating can enhance the cyclogenesis process in two ways. First, saturated conditions can effectively reduce the static stability and enhance the vertical penetration of the circulation of the upper- and lower-boundary PV anomalies. Second, a maximum of diabatic heating produces a positive (negative) PV anomaly upshear (downshear) along the absolute vorticity vector (Raymond 1992). If the maximum of diabatic heating is located in the mid-troposphere, this generally leads to the generation of a positive PV anomaly in the lower troposphere and a negative PV anomaly in the upper-troposphere. The vertical gradient of the heating is directly proportional to the amount of PV produced (Stoelinga 1996).

Previous studies have found that the impact of a lower-tropospheric diabatically generated PV anomaly on cyclogenesis varies from case to case. In some instances, this anomaly is the primary contribution to the cyclogenesis (Reed et al. 1992) and can facilitate the phase locking and mutual amplification of the upper- and lower-boundary PV anomalies (Stoelinga 1996). However, in other cases, the diabatic anomaly provides only a minor contribution to the cyclone strength, or can actually inhibit phase-locking of the upper and lower-boundary PV anomalies (Davis 1992).

Diabatically-produced cyclonic PV anomalies can also contribute to the moisture transport into a cyclone. Lackmann (2002) found that a diabatically produced PV anomaly along a cold front contributed between 15% and 40% of the strength of a low-level jet event in the southern U.S. It serves to follow that a lower-tropospheric, diabatically produced positive PV anomaly associated with a cyclone could play an important role in the moisture transport into the system.

The so-called “surprise snowstorm” of 24–25 January 2000 produced heavy snow from the Carolinas northward into the mid-Atlantic region, including the storm-total snowfall record at Raleigh-Durham, NC (RDU) of 51.5 cm (20.3 in., NCDC 2000). A Barnes objective analysis (Koch et al. 1983) of liquid-equivalent precipitation totals from 24–26 January 2000 reported by National Weather Service cooperative observers shows that more than 1 in. of precipitation fell across the central and eastern Carolinas and southeast Virginia (Fig. 1). Maximum amounts exceeded 3 in. across eastern South Carolina and southeastern North Carolina. In contrast, the 48-h precipitation forecast from the National Centers for Environmental Prediction (NCEP) Eta model is significantly lighter, with amounts greater than 0.5 in. confined to the immediate coastal area of North Carolina (Fig. 2).

Previous studies have attributed the poor operational model forecast of this event to sensitivity to initial conditions (Zhang et al. 2002; Langland et al. 2002), and the limits of mesoscale predictability in the presence of moist processes (Zhang et al. 2003), while others have focused on the benefits of ensemble forecasting (Buzzia and Chessa 2002). Here, we seek to pinpoint the role of LHR produced by an area of antecedent precipitation in the westward movement of the precipitation shield in the Carolinas and mid-Atlantic.

2. MOTIVATION AND HYPOTHESIS

An area of antecedent precipitation developed over the lower Mississippi River Valley and southeast United States prior to 12 UTC 24 January, immediately before rapid deepening of the cyclone occurred between 12 UTC 24 Jan. and 00 UTC 25 Jan (From this point forward, date and time will be referenced as DD/HH, e.g. 24/00 is 00 UTC 24 Jan.). Radar imagery at 24/09 shows a large band of moderate to heavy precipitation from the northern Gulf of Mexico northeastward across southeastern Alabama to central Georgia (Fig. 3). Observations of 6-h precipitation ending at 12 UTC show that rainfall exceeded 0.40 in. over portions of Alabama and Georgia, with maximum amounts approaching or exceeding 1 in. This precipitation was poorly forecast by the 24/00 run of the Eta model, with the 6-h precipitation forecast ending at 24/12 indicating less than 0.25 in. over eastern Alabama and western Georgia where 0.40–1.25 in. was observed. It is clear that the Eta model was unable to resolve the significant

* *Corresponding author address:* Michael J. Brennan, North Carolina State University, Dept. of Marine, Earth and Atmospheric Sciences, Raleigh, NC 27695; email: mike_brennan@ncsu.edu

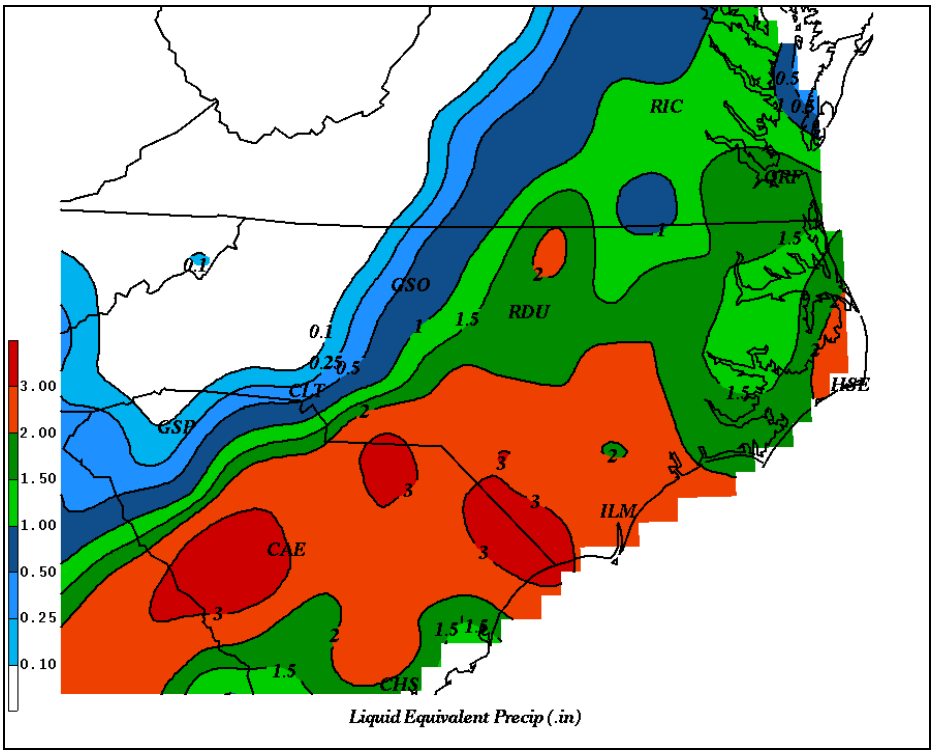

Figure 1. Observed liquid-equivalent precipitation (inches) from NWS cooperative observers from 24–26 January 2000.

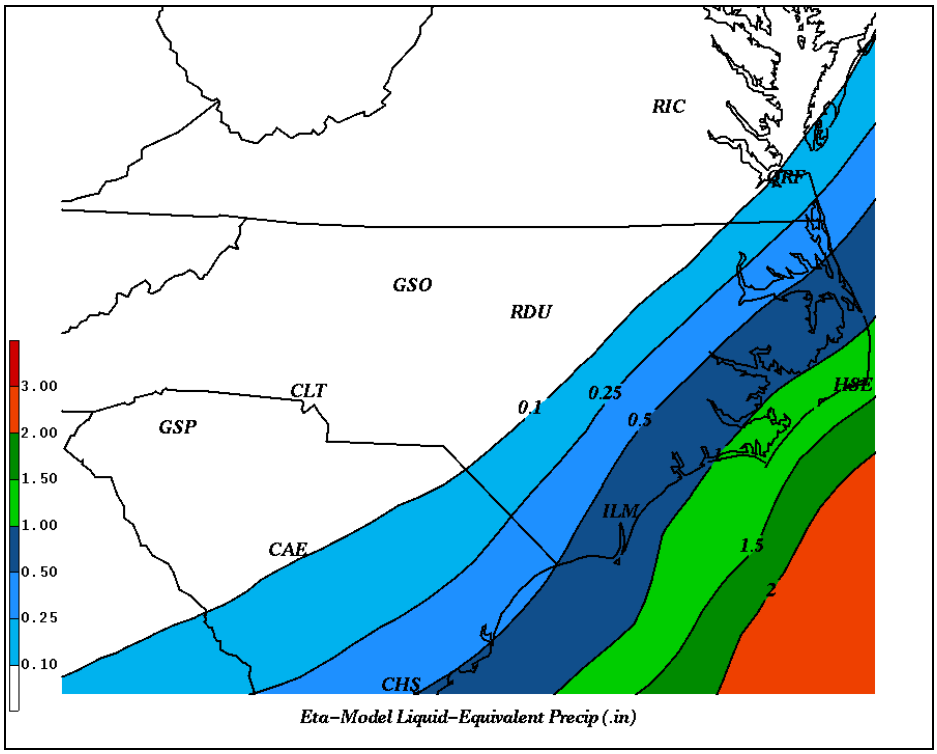

Figure 2. As in Fig. 1, except 48-h forecast from 00 UTC 24 January 2000 Eta Model run ending at 00 UTC 26 January 2000.

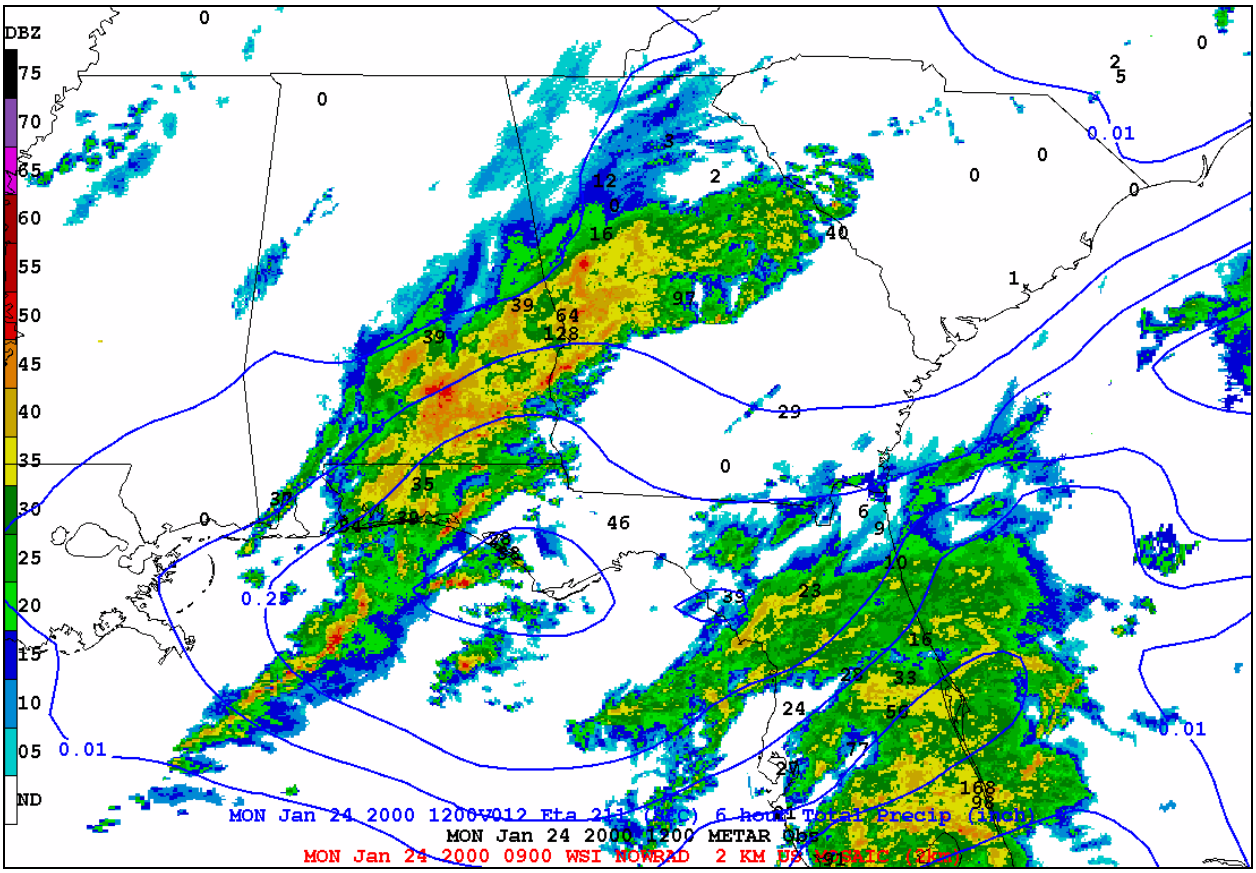

Figure 3. Radar mosaic valid at 09 UTC 24 January 2000 with observed 6-h precipitation totals ending at 12 UTC 24 January 2000 in hundredths of inches (black numerals) and 6-h precipitation forecast from Eta model ending at 12 UTC 24 January 2000 (blue contours, in.)

area of antecedent precipitation over the southeastern U.S. prior to rapid cyclogenesis. Therefore, the Eta model would be unable to properly predict the formation of the diabatic PV maximum in the lower-troposphere produced by the antecedent precipitation. We hypothesize that this PV maximum and its induced circulation is the *critical* feature responsible for low-level moisture transport into the Carolinas and Virginia during the cyclone event, and that the inability of the Eta model (or any model) to properly resolve this feature is a major factor in the poor forecast of the cyclone evolution and its precipitation distribution.

To test this hypothesis, we will compute a PV budget from a mesoscale model simulation of this event to determine if the low-level PV anomaly is indeed diabatically produced. Then, we will perform a piecewise PV inversion of this lower-tropospheric PV anomaly to quantify its impact on the moisture flux into the Carolinas and mid-Atlantic.

3. MESOSCALE MODEL SIMULATION

This case was simulated using version 3.5 of the fifth-generation Pennsylvania State University-National Center for Atmospheric Research (NCAR) mesoscale model (MM5, Grell et al. 1994).

Initial attempts to simulate this case by initializing MM5 prior to the development of the antecedent precipitation were unsuccessful despite varying initial conditions, model grid spacing, and physical parameterizations. Regardless of the model configuration, no simulation initialized prior to the development of the antecedent precipitation was able to properly reproduce the cyclone evolution and precipitation distribution.

Ultimately, a successful control simulation (CTRL) was achieved by initializing MM5 after the development of the antecedent precipitation. Initial data for this simulation was provided by the Rapid Update Cycle (RUC, Benjamin et al. 1998) model analysis at 24/09 and run for 39 hours through 26/00. Subsequent RUC analyses were used every three hours throughout the simulation to provide lateral boundary conditions. The model domain used in this study has a horizontal grid spacing of 36 km and 37 vertical sigma levels, covering much of the eastern United States and adjacent coastal waters (Fig. 4).

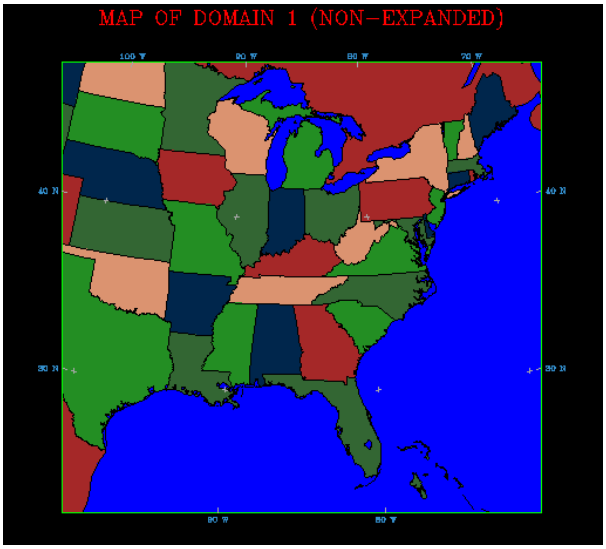

Figure 4. MM5 domain used in simulations.

Physical parameterizations chosen for this simulation were the Reisner mixed-phase explicit moisture scheme (Reisner et al. 1998), the Grell cumulus parameterization (CP) scheme (Grell et al. 1994), the Blackadar high-resolution planetary boundary layer scheme (Zhang and Anthes 1982), and the Dudhia cloud radiation scheme (Dudhia 1989). Climatological snow-cover data were used. Sea-surface temperature (SST) data on a 14-km grid derived from 8-km grid-spacing SST observations generated every 48 h over North America and adjacent waters were used as the lower-boundary condition.

The MM5 source code was modified to directly output the instantaneous temperature tendencies from the explicit moisture and cumulus parameterization schemes. This was done to quantify the impact of the LHR produced by the explicit moisture and CP schemes on the PV distribution.

A second simulation was also run, initialized from the 24/00 Eta model, which was unable to properly predict the Antecedent Precipitation feature discussed in the previous section. This simulation will be referred to as the "NOAP" simulation. Results from NOAP will be compared to those from CTRL to examine the impact of the antecedent precipitation on the cyclone evolution and the precipitation distribution.

4. PV BUDGET

A PV budget from simulation CTRL was calculated based on the methods outlined in Raymond (1992), Cammas et al. (1994), and Lackmann (2002). It provides a means to identify lower tropospheric PV anomalies that have been enhanced by LHR and determine whether LHR is capable of producing a given PV anomaly. The budget was computed using the MM5 output every three hours and using LHR from the explicit precipitation and CP schemes.

At 24/12, LHR at 700 hPa is maximized over central and southwest Georgia, with values exceeding 180 x 10^{-5} K s^{-1} (Fig. 5a). A PV maximum in the 700–900 hPa layer is co-located with the LHR maximum with values of 1–1.25 potential vorticity units (PVU; where 1 PVU = 1.0 x 10^{-6} m^3 s^{-1} K kg^{-1}) over southwestern Georgia. By 24/15, the strongest 700-hPa LHR has moved north into eastern South Carolina, with maximum values of 180 x 10^{-5} K s^{-1} (Fig. 5b). Maximum PV values are now between 1.5 and 2 PVU over northeastern Georgia. The PV maximum continues to intensify and move eastward at 24/18 (Fig. 5c), and by 25/00 the strongest LHR has shifted northeastward into eastern North Carolina, with the PV increasing to over 2.5 PVU offshore of southern North Carolina, extending northeastward offshore to east of Cape Hatteras. (Fig. 5d)

A cross section at 24/15 from 32.5°N 86°W to 30.5°N 79°W shows a distinct PV maximum centered near 925 hPa with a magnitude greater than 2 PVU centered upstream along the absolute vorticity vector from a LHR maximum centered near 700 hPa (Fig. 6).

Over the period from 24/12–25/00 a lower tropospheric PV maximum increased in size and magnitude over the southeastern United States, tied closely to a 700-hPa LHR maximum that moved across the region. PV values increased from 1.25 to 2.5 PVU in the 12-h period. This PV maximum developed upstream of the absolute vorticity vector from a LHR maximum, consistent with the findings of Raymond (1992), suggesting that the PV maximum was not simply advected into the region, but was produced *in-situ* by the latent heating occurring due to precipitation processes in the region.

5. PV INVERSION

To quantify the impact of this diabatic PV feature on the moisture transport and the cyclone evolution, nonlinear piecewise PV inversion was performed based on the methodology outlined in Davis and Emanuel (1991). The inversion method solves for balanced fields of geopotential (Φ) and streamfunction (ψ) using perturbation values of Ertel's PV on the model interior as well as upper- and lower-boundary potential temperature (θ). To compute background fields of PV, θ, Φ, and ψ for the inversion, daily output from a 14-day MM5 simulation was averaged at each pressure level. The simulation was run from 17–31 January 2000, with initial and boundary conditions supplied from the 2.5° × 2.5° NCEP/NCAR reanalysis (Kalnay et al. 1996). Anomaly values of PV, θ, Φ, and ψ were defined as the difference between the instantaneous value and the background field.

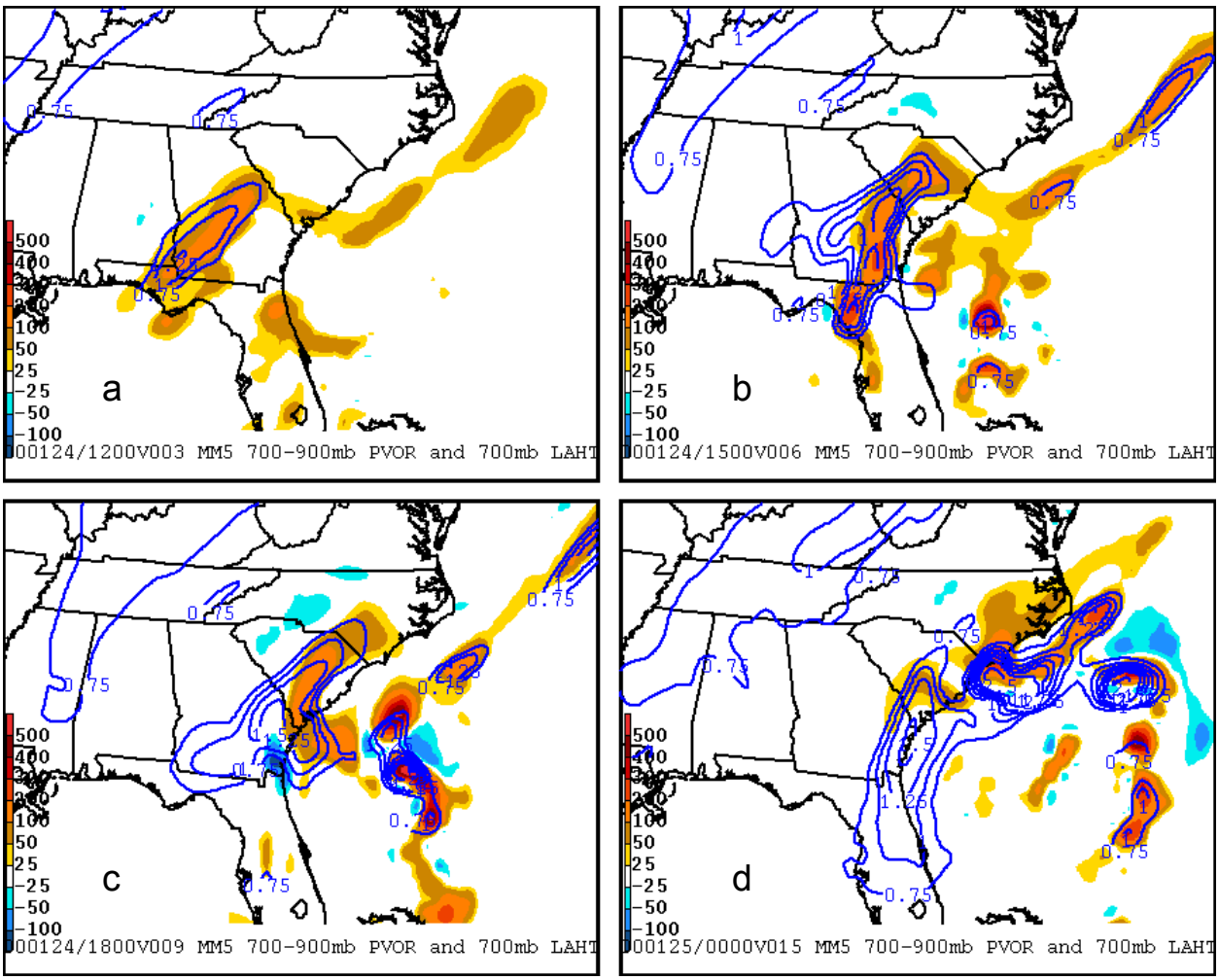

Figure 5. 700-900 hPa PV (blue contours, PVU) and 700-hPa temperature tendency (x 10^{-5} K s^{-1}) from CTRL simulation explicit precipitation and cumulus parameterization schemes at (a) 12 UTC, (b) 15 UTC, (c) 18 UTC 24 Jan., and (d) 00 UTC 25 Jan. Warm (cool) color shading indicates heating (cooling) according to color scale. The line A-A' in panel b indicates the location of the cross section shown in Fig. 6.

For the purposes of inversion the PV distribution was divided into four pieces. Cyclonic (anticyclonic) PV anomalies below 600 hPa were inverted with lower-boundary warm (cold) θ anomalies, as were cyclonic (anticyclonic) PV anomalies above 600 hPa and upper-boundary cold (warm) θ anomalies. At the lateral boundaries, perturbation values of Φ and ψ of the same sense (e.g. Φ, ψ < 0 for cyclonic PV) were specified at the particular levels where PV was being inverted and were set to zero elsewhere. Results presented here are from the PV inversion conducted at 25/00.

At 25/06, the cyclone in the MM5 simulation was located southeast of North Carolina with a central pressure of 991 hPa, and widespread precipitation was occurring over much of the Carolinas at this time (Fig. 7). Figure 8 shows the 800-hPa moisture flux from the balanced flow associated with the cyclonic PV anomaly below 600 hPa and the warm lower-boundary θ anomaly from CTRL. The flux was computed by multiplying the balanced flow from the inversion by the mixing ratio from the MM5 simulation.

$$\vec{F}_m = q(\vec{V}_B) \qquad (1)$$

where *q* is the mixing ratio and

$$\vec{V}_B = (-\frac{\partial \varphi}{\partial y} i + \frac{\partial \varphi}{\partial x} j) \qquad (2)$$

where $\boldsymbol{V_B}$ is the balanced flow computed from the balanced streamfunction field from the PV inversion.

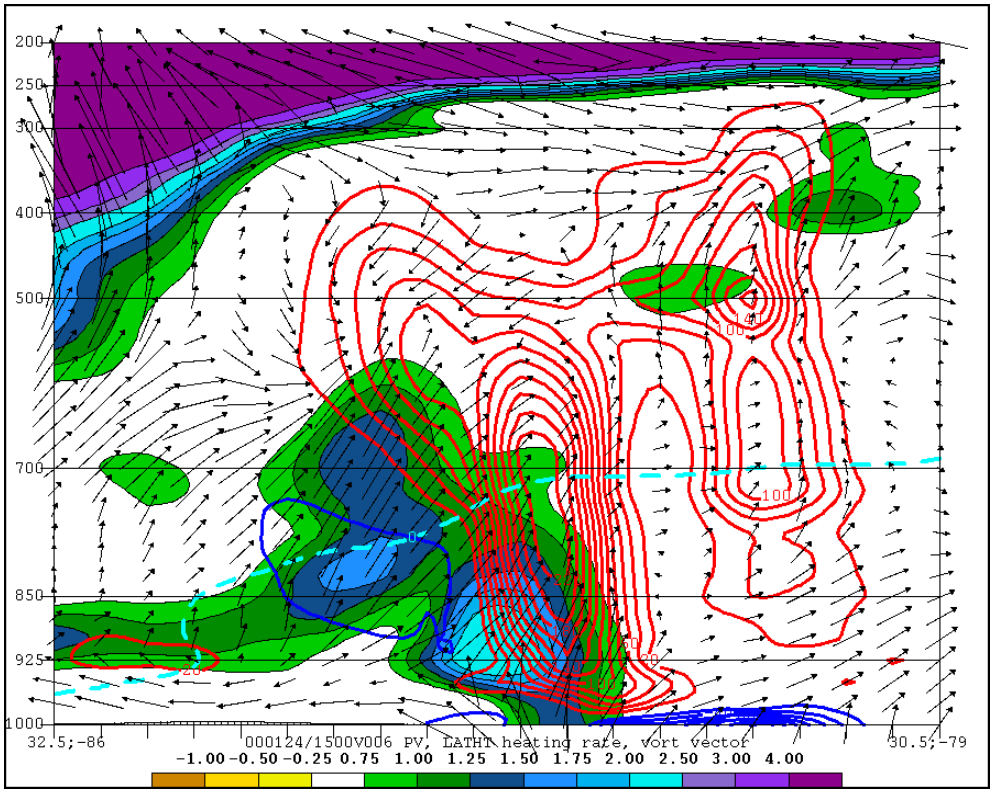

Figure 6. CTRL simulation cross-section from 32.5°N 86°W to 30.5°N 79°W at 15 UTC 24 Jan. showing PV (shaded, PVU, see color bar for scale), temperature tendency from model precipitation schemes, positive (negative) values in red (blue) contoured every 20 x 10^{-5} K s^{-1}, and absolute vorticity vectors (black arrows).

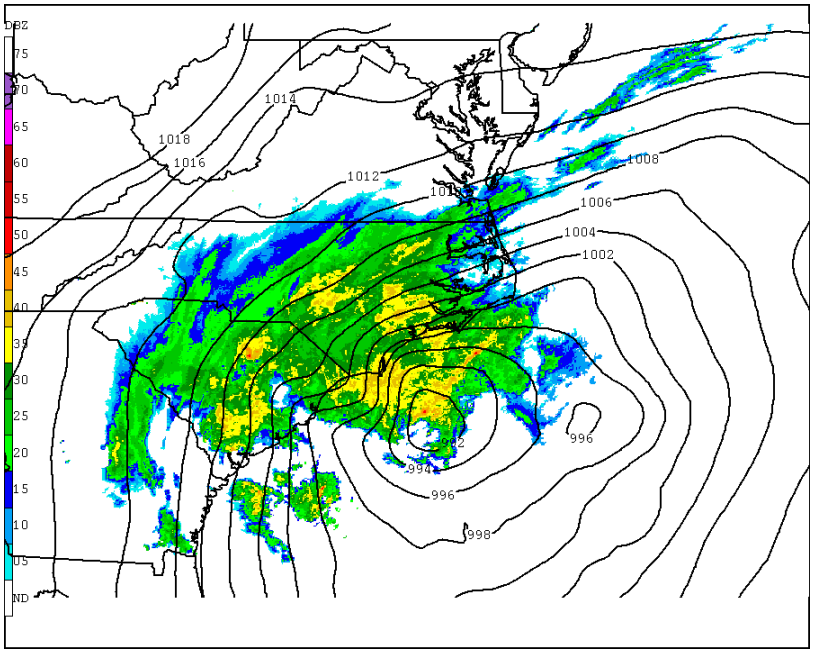

Figure 7. Mean sea-level pressure from CTRL (black contours every 2 hPa) and observed radar reflectivity valid at 00 UTC 25 January 2000.

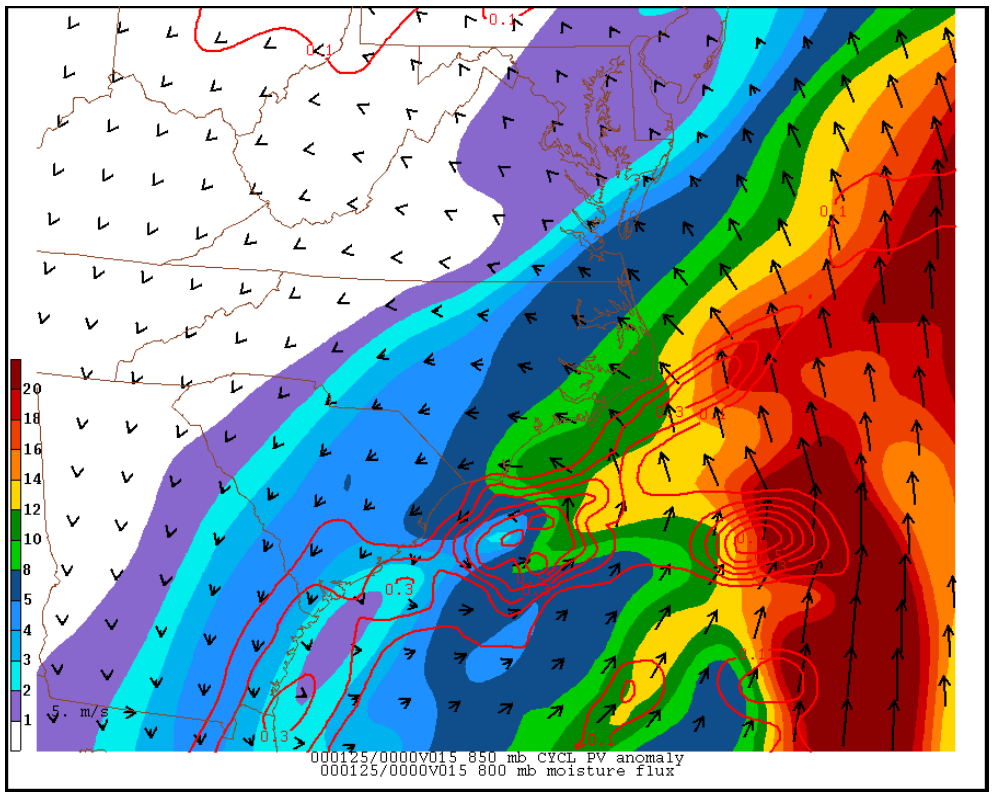

Figure 8. 800-hPa moisture flux (x 10^{-4} m s^{-1} shaded) and moisture flux vectors (x 10^{-4} m s^{-1} black arrows) and 850-hPa cyclonic PV anomaly (red contours every 0.2 PVU) from CTRL valid at 00 UTC 25 January 2000.

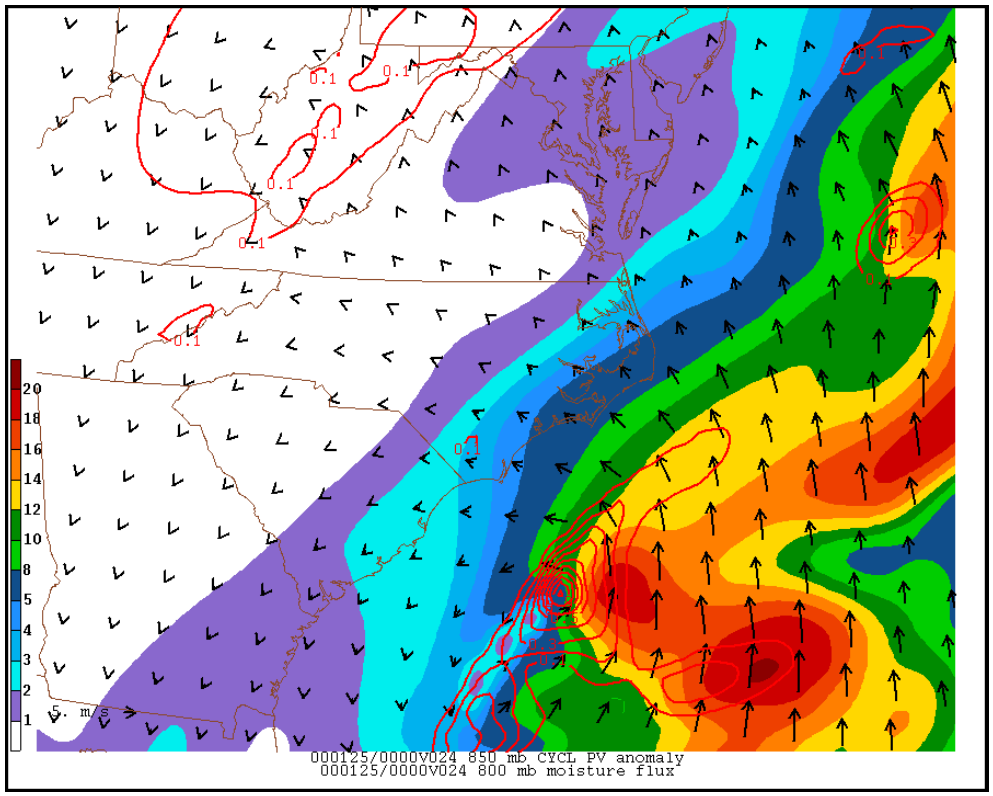

Figure 9. As in Fig. 8, except from NOAP.

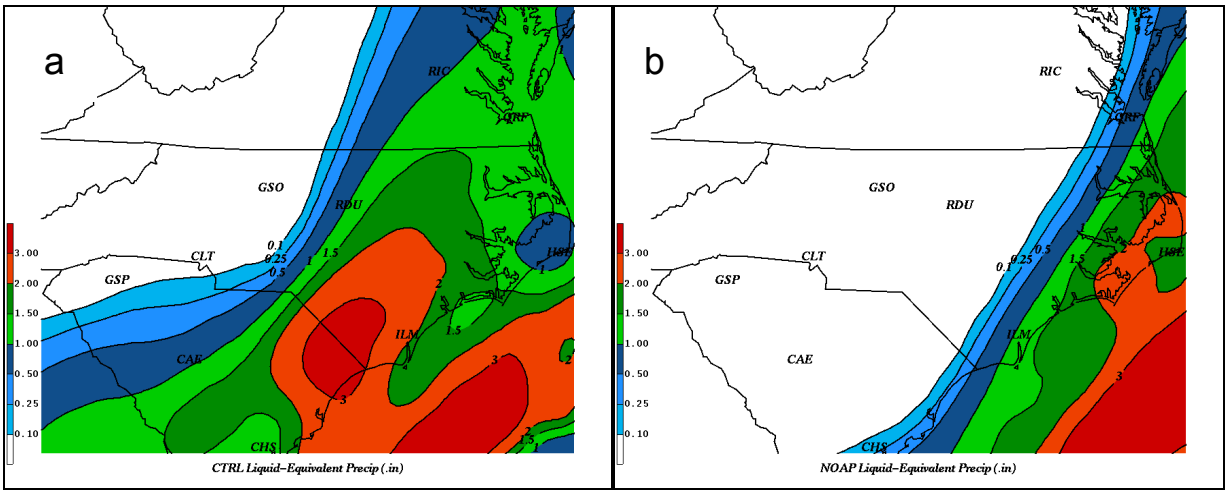

Figure 10. Liquid-equivalent precipitation (inches) from (a) CTRL and (b) NOAP simulations.

Perturbation PV values at 850 hPa are greater than 0.6 PVU offshore of the Carolinas, with flux vectors indicating cyclonic flow transporting moisture inland to the western Piedmont of the Carolinas north of the PV anomaly center.

The same PV inversion was performed on output from simulation NOAP at 25/00. It is clear that the corresponding moisture flux is much weaker and is maximized farther offshore when compared to CTRL (Fig. 9). While the 850-hPa PV anomaly is still near 06 PVU in NOAP, it is much smaller and farther offshore than CTRL, consistent with the weaker moisture flux.

These results are consistent with the precipitation produced by the respective simulations. In CTRL, the 1 in. precipitation contour extends westward into central North Carolina (Fig. 10a). While the total precipitation is still too light when compared to observations (Fig. 1), it does show a significant improvement over the operational Eta model forecast (Fig. 2). Not surprisingly, the NOAP simulation confines all precipitation greater than 0.1 in. to the coastal areas of the Carolinas and Virginia (Fig. 10b). This is very similar to the precipitation produced by the operational Eta model (Fig. 1).

6. CONCLUSIONS AND FUTURE WORK

We have shown that a diabatically generated PV anomaly was produced by a large area of antecedent precipitation that developed across the southeastern U.S. on 24 Jan. 2000, prior to the rapid cyclogenesis that occurred later that day off the southeast U.S. coast. This PV anomaly was strongly linked to the low- and mid-level moisture transport into the Carolinas and Virginia, as seen in the results of the piecewise PV inversion.

A mesoscale model simulation (CTRL) initialized after the early precipitation feature was underway was significantly more successful in simulating the cyclone's evolution and precipitation distribution than the Eta model run from 00 UTC 24 Jan., suggesting that this precipitation feature was a critical factor in the Eta model's poor forecast of this event. PV inversion from simulation NOAP shows that a much weaker lower-tropospheric PV anomaly developed too far offshore compared CTRL, leading to a much weaker moisture flux and lower precipitation totals in the Carolinas and Virginia in NOAP relative to CTRL and observations. This provides a direct link between the diabatic PV feature associated with the antecedent precipitation and the inland penetration of the PV field

The next question that presents itself is why the Eta model was unable to properly forecast the development of a large-scale antecedent precipitation region that developed over the heart of the data network in the 6–12 h timeframe? Future work will include investigation of the nature of this early precipitation feature. Preliminary findings indicate that elevated and/or slantwise convection may have played a role in its development.

Ultimately, it is our hope that improving the representation of mesoscale precipitation systems in operational numerical weather prediction models will lead to better forecasts in high-impact weather events such as the case described here.

7. ACKNOWLEDGEMENTS

This research was funded by NSF grant ATM-0079425 and NOAA CSTAR grant, NA-07WA0206. We thank Dr. Chris Davis for providing the piecewise PV inversion code. The State Climate Office of North Carolina provided liquid equivalent precipitation totals used in Figure 1. The Unidata program provided much of the meteorological data used in this study. The MM5 model was provided by NCAR, which is funded by NSF. The gridder code for MM5 was developed at the University of Utah by Prof. Jim Steenburgh and Daryl Onton. Thanks to Drs. Jimy Dudia and Jack Kain for assistance with outputting individual temperature tendency terms from MM5.

8. REFERENCES

Benjamin, S. G., J. M. Brown, K. J. Brundage, B. E. Schwartz, T. G. Smirnova, T. L. Smith, L. L. Morone, 1998: RUC-2 - The Rapid Update Cycle Version 2. NWS Technical Procedure Bulletin No. 448. NOAA/NWS, 18 pp. [Available online at http://205.156.54.206/om/tpb/448.htm].

Bosart, L. F., 1981: The Presidents' Day snowstorm of 18–19 February 1979: A sub-synoptic scale event. *Mon. Wea. Rev.,* **109,** 1542–1566.

Buzzia, R., and P. Chessa, 2002: Prediction of the U.S. storm of 24–25 January 2000 with the ECMWF ensemble prediction system. *Mon. Wea. Rev.,* **130,** 1531–1551.

Cammas, J.-P., D. Keyser, G. M. Lackmann, and J. Molinari, 1994: Diabaitc redistribution of potential vorticity accompanying the development of an outflow jet within a strong extratropical cyclone. *Proc. Int. Symp. on the Life Cycles of Extratropical Cyclones,* Vol. II, Bergen, Norway, Geophysical Institute, University of Bergen. 403–409.

Coleman, B. R., 1990. Thunderstorms above frontal surfaces in environments without positive CAPE: Part I: A climatology. *Mon. Wea. Rev.,* **118,** 1103–1121.

Davis, C. A., 1992a: A potential-vorticity diagnosis of the importance of initial structure and condensational heating in observed extratropical cyclogenesis. *Mon. Wea. Rev.,* **120,** 2409–2428.

———, and K. A. Emanuel, 1991: Potential vorticity diagnostics of cyclogenesis. *Mon. Wea. Rev.,* **119,** 1929–1953.

Dudhia, J., 1989: Numerical study of convection observed during the Winter Monsoon Experiment using a mesoscale two-dimensional model. *J. Atmos. Sci.,* **46,** 3077–3107.

Grell, G. A., J. Dudhia, and D. S. Stauffer, 1994: A description of the fifth-generation Penn State/NCAR mesoscale model (MM5). NCAR Tech. Note, NCAR/TN-3981STR, 122 pp.

Hoskins, B. J., M. E. McIntyre, and A. W. Robertson, 1985: On the use and significance of isentropic potential vorticity maps. *Quart. J. Roy. Meteor. Soc.,* **111,** 877–946.

Kalnay, E., and Coauthors, 1996: The NCEP/NCAR 40-Year Reanalysis Project, *Bull. Amer. Meteor. Soc.,* **77,** 437–471.

Koch, S. E., M. desJardins, and P. Kocin, 1983: An interactive Barnes objective map analysis scheme for use with satellite and conventional data. *J. Climate Appl. Meteor.,* **22,** 1487–1503.

Lackmann, G. L., 2002: Cold-frontal potential vorticity maxima, the low-level jet, and moisture transport in extratropical cyclones. *Mon. Wea. Rev.,* **130,** 59–74.

———, and J. G. Gyakum, 1999: Heavy cold-season precipitation in the northwestern United States: Synoptic climatology and an analysis of the flood of 17–18 January 1986. *Wea. Forecasting,* **14,** 687–700.

Langland, R. F., M. A. Shapiro, and R. Gelaro, 2002: Initial condition sensitivity and error growth in forecasts of the 25 January 2000 east coast snowstorm. *Mon. Wea. Rev.,* **130,** 957–974.

NCDC, 2000: *Storm Data*, Vol. 42.

Raymond, D. J., 1992: Nonlinear balance and potential-vorticity thinking at large Rossby number. *Quart. J. Roy. Meteor. Soc.,* **118,** 987–1015.

Reed, R. J., M. T. Stoelinga, and Y.-H. Kuo, 1992: A model-based study of the origin and evolution of the anomalously high potential vorticity in the inner region of a rapidly deepening marine cyclone. *Mon. Wea. Rev.,* **120,** 893–913.

Resiner, J., R. M. Rasmussen, and R. T. Bruintjes, 1998: Explicit forecasting of supercooled liquid water in winter storms using the MM5 mesoscale model. *Quart. J. Roy. Meteor. Soc.,* **124,** 1071–1107.

Stoelinga, M. T., 1996: A potential-vorticity based study of the role of diabatic heating and friction in a numerically simulated baroclinic cyclone. *Mon. Wea. Rev.,* **124,** 849–874.

Tracton, M. S., 1973: The role of cumulus convection in the development of extratropical cyclones. *Mon. Wea. Rev.,* **101,** 573–592.

Zhang, D.-L., and R. A. Anthes, 1982: A high-resolution model of the planetary boundary layer—Sensitivity tests and comparisons with SESAME-79 data. *J. Appl. Meteor.,* **21,** 1594–1609.

Zhang, F., C. Snyder, and R. Rotunno, 2002: Mesoscale predictability of the "surprise" snowstorm of 24–25 January 2000. *Mon. Wea. Rev.,* **130,** 1617–1632.

———, C. Snyder, and R. Rotunno, 2003: Effects of moist convection on mesoscale predictability. *J. Atmos. Sci.,* **60,** 1173-1185.